Downloaded from SAE International by Wayne State University, Friday, September 16, 2016

SAE INTERNATIONAL

Simulation of Dual-Fuel-CI and Single-Fuel-SI Engine Combustion Fueled with CNG

2016-01-0789
Published 04/05/2016

Apoorv P. Talekar and Ming-Chia Lai
Wayne State University

Ke Zeng and Bo Yang
Xian Jiaotong University

Marcis Jansons
Wayne State University

CITATION: Talekar, A., Lai, M., Zeng, K., Yang, B. et al., "Simulation of Dual-Fuel-CI and Single-Fuel-SI Engine Combustion Fueled with CNG," SAE Technical Paper 2016-01-0789, 2016, doi:10.4271/2016-01-0789.

Copyright © 2016 SAE International

Abstract

With increasing interest to reduce the dependency on gasoline and diesel, alternative energy source like compressed natural gas (CNG) is a viable option for internal combustion engines. Spark-ignited (SI) CNG engine is the simplest way to utilize CNG in engines, but direct injection (DI) Diesel-CNG dual-fuel engine is known to offer improvement in combustion efficiency and reduction in exhaust gases. Dual-fuel engine has characteristics similar to both SI engine and diesel engine which makes the combustion process more complex. This paper reports the computational fluid dynamics simulation of both DI dual-fuel compression ignition (CI) and SI CNG engines. In diesel-CNG dual-fuel engine simulations and comparison to experiments, attention was on ignition delay, transition from auto-ignition to flame propagation and heat released from the combustion of diesel and gaseous fuel, as well as relevant pollutants emissions. Injection timing for diesel pilot was changed in a test matrix and the most efficient and least pollutant producing cases were selected and simulation results were correlated to the experimental data for those cases. The possible end-gas auto-ignition-like processes under certain test conditions like PREmixed Mixture Ignition in the End-gas Region (PREMIER) were also demonstrated. SI CNG lean burn engine tests and simulations were directed to check the ignitability, combustion stability, heat release rate for different spark energy values. The results show that a combined approach of using both chemical kinetics and G-equation formulations in RANS is capable of capturing most of the physical-chemical processes in both the dual-fuel CI and SI engine combustions.

Introduction

With increasing concerns about air pollution, especially the particulate matter (PM) emissions of diesel engine, more stringent regulations to limit engine emissions were legislated. In recent years, as a result, many methods have been proposed to simultaneously reduce PM and nitrogen oxides (NO_x) emissions in diesel engine. Using alternative fuels and gaseous fuels in existing diesel engine has been proved to be one of the most practical ways to reduce the harmful emissions[1, 2, 3, 4]. Natural gas is available in great quantities with considerably cheap price in many parts of the world and also has the advantage of low emissions of all carbonaceous emissions. Moreover, its relatively high auto-ignition temperature is a great advantage over other gaseous fuels, because the high compression ratio of most conventional direct injection diesel engine can be maintained when natural gas is employed [5]. As a result, natural gas is likely used as the primary fuel in a diesel engine which is referred to as pilot ignited natural gas/diesel dual-fuel engine. In recent years, extensive research has been conducted to investigate the effects of various parameters on the performance, combustion and emissions of natural gas/diesel dual-fuel engine.

Another recent emphasis on CO_2 emissions reduction also encourages natural gas use in internal combustion engines. Natural gas has methane as a major component and propane, iso-butane in less quantity hence carbon to hydrogen ratio is less compared to the diesel. As a result, natural gas is likely used as the displacement fuel in a diesel engine as pilot ignited natural gas/diesel dual-fuel engine, or in a gasoline engine, to take advantages of the various benefits of natural gas. In recent years, extensive research has been conducted to investigate the effects of various parameters on the performance, combustion and emissions of natural gas-fueled engine. In order to meet these demands, we need to accurately predict the ignition and combustion of natural gas inside engines, in dual-fuel and SI combustion modes.

Downloaded from SAE International by Wayne State University, Friday, September 16, 2016

Zoldak et al. [6][7] used reduced ERC n-heptane mechanism with 29 species and 52 reactions combined with NO_x mechanism (4 species and 12 reactions). They used a sector mesh with one nozzle and dual injection for diesel liquid which showed improvement in fuel efficiency and reduction in particulate matter emission compared to diesel only operation. The authors also found that the rate of pressure rise is too sensitive to injection timing.

Papagiannakis, et al. [8,9] employed a comprehensive two-zone phenomenological model to examine the effects of pilot fuel quantity and pilot injection timing on the dual-fuel engine performance and emissions, and then validated the model with experiment in a premixed dual-fuel engine. They reported that simultaneously increase of the pilot fuel quantity accompanied with an increase of its injection timing results in an improvement of the engine efficiency (increase) and CO emissions (decrease) while it has a negative effect (increase) of NO_x emissions.

Kong and Reitz formulated model for diesel dual-fuel operation using SHELL v1 auto-ignition model which uses equilibrium concentration of seven major species fuel, O_2, N_2, CO_2, H_2, H_2O and CO [10,11]. SHELL model [12] uses a simplified reaction mechanism to simulate the auto-ignition of hydrocarbon fuels. The mechanism consists of eight generic reactions and five generic species. Ignition delay prediction using this model is known to be sensitive to preexponential factor in the rate constant of the reaction. Liang and Reitz developed a model which uses G-equation based turbulent combustion model and also detailed chemical kinetics for the post-flame calculation for SI CNG engine [13, 14, 15]

Abagnale et.al. [14] used the self-ignition of diesel fuel which is governed by the Stringer relationships [17] for the ignition delay and the diesel combustion model employed for a full engine cycle calculation consists of the classical one step kinetic mechanism of fuel oxidation within a finite rate eddy dissipation approach [18]. The natural gas combustion is approximated by a 100% methane oxidation process with a two-step mechanism in KIVA-3V software [19]. They found that low NG substitution combustion is characterized by the delayed ignition of the major fraction of the fuel. For higher NG substitution rate the faster and advanced combustion development with steeper pressure and heat release curve was noted. Mattarelli et.al. [20] coupled the partially premixed reactor spray combustion model (PaSR) and the flame propagation model in KIVA-3V to simulate dual-fuel operation. Diesel oil surrogate, a blend of n-heptane and toluene was used and natural gas was represented by the mixture of methane (>90%), ethane, propane and n-butane. The resulting mechanism included 81 species and 421 reaction. With the reduction in amounts of CO and CO_2 they found the significant increase in NO and concluded that it can be reduced by different SOI.

In this paper detailed chemistry auto-ignition model is used with G-equation model to model the combustion of single-fuel SI and diesel-CNG CI dual-fuel engines.

Experimental Set-Up for Diesel Dual-fuel Engines

A Turbo-charged 2.8 liter diesel engine was equipped with a sequential natural gas manifold injection system in order to operate the diesel engine in dual-fuel mode [21]. The effects of natural gas injection timing on the combustion performance and emissions (NO_x, HC, CO and PM) of the dual-fuel engine, with special attention to the combustion performance under low and part engine loads were used to compare with the simulation. Table 1 shows the engine specifications and Table 2 elaborates the properties of fuel used for the experiment.

Table 1. CI Engine Specifications

Item	characteristics
Type	4-stroke, common rail injection
Cylinder number	4
Bore X stroke	93mm×102mm
Compression ratio	17.2:1
Injection system	Common rail
Max. injection pressure	145Mpa
Diesel direct-injection nozzle	6×0.137mm
Natural gas injection nozzle	1×3.0mm
Valve timing	Opening Closing
Intake	24°BTDC 55°ABDC
Exhaust	54°BBDC 26°ATDC

Table 2. Test Fuel Properties

Fuel properties	Diesel	Natural
Low heating value (MJ/kg)	42.8	50.0
Cetane / Octane number	52.5/-	-/130
Auto-ignition temperature (℃)	250	650
Stoichiometric air-fuel ratio	14.69	17.2
Carbon content / % by mass	87	75

Table 3. Testing Conditions for Dual-fuel Engine

Case	SOI (CA)	Engine Speed (rpm)	BMEP (MPa)	IMEP (MPa)	Diesel Sub. Rate %	CNG (kg/hr)	Diesel (kg/hr)	Over-all λ
1	-23	1600	1.040	1.349	82.88	4.050	0.470	1.8
2	-21	1600	1.060	1.156	82.47	4.051	0.482	1.78
3	-15	1600	0.965	0.999	82.38	4.072	0.484	1.75
4	-11	1600	0.866	0.975	82.90	4.047	0.469	1.78
5	-9	1600	0.729	0.857	83.19	4.056	0.485	1.78
6	-8	1600	0.480	0.682	68.87	4.139	0.855	1.5
7	-5	1600	0.475	0.490	82.82	4.000	0.472	1.79

Natural gas injection timing is defined as the start injection crank angle at which the natural gas injection signal is sent to natural gas injectors by the dual-fuel ECU and it was varied from -500° CA to -240° CA aTDC and the other parameters were not changed in order to explore the effects of natural gas injection timing on the combustion characteristics and emissions. The three engine test operation conditions, under low-, part- and high-load are summarized in Table.3.In case 6 the pilot diesel injection timing was fixed at 8 CA bTDC for the purpose of simultaneous reducing cylinder pressure rise rate and NO_x emissions compared with that under pure diesel operation modes. . For this case pilot diesel fuel quantity is doubled and hence diesel substitution rate is 68.87%, less than rest of the cases.

Downloaded from SAE International by Wayne State University, Friday, September 16, 2016

Experimental Set-Up for SI-CNG Engine

The combustion data of a four-valve 0.5 liter engine with CNG injection upstream of the intake pipe was used to compare with the simulation [22]. The ignition energy was varied between 65 mJ and 240 mJ at fixed lambda values to look for gains in thermal efficiency, as shown in the Table 5; two lambda values were chosen (1.25 and 0.9) for simulation study. These values are the most lean and rich cases in the experimental test matrix respectively.

Table 4. SI Engine Specifications

Configuration	Single cylinder
Displacement	500cc
Compression Ratio	10.2:1
Valve Configuration	DOHC
Valves per Cylinder	4
Bore x Stroke	86mm x 86mm
Fuel System	PFI CNG system retrofitted
Injection pressure	7.6 bar

Table 5. Testing Conditions for SI Engine

MAP	0.5 bar
Injection timing	300 CA bTDC
Ignition timing	10 CA bTDC
Lambda	1.25, 0.9
Spark Discharge Energy	65mJ,180mJ, 240mJ

Simulation Model Set-Up

Simulations of SI-CNG and diesel-CNG dual-fuel engine were performed using 3D CFD software CONVERGE. RNG (Renormalization Group) k-ε model was used to model turbulence in both SI and diesel-CNG dual-fuel engine due to the numerical stability of this two equation RANS model. For dual-fuel engine simulation whole combustion chamber was modeled (360°) with injector having 6 holes. For SI engine whole engine with 4 valves and two ports was modeled with spark plug at the center of the cylinder head.

Chemical Mechanism

For diesel dual-fuel engine combustion n-heptane reduced mechanism developed by Lawrence Livermore National Laboratory (LLNL) [23][24] was used. It includes 159 chemical species and 1282 reversible reactions. GRI-MECH 3.0 was used for the modeling of the combustion of CNG in SI engine. This mechanism comprises 53 species and 325 elementary chemical reactions [25]. To focus on the effect of pilot injection timing, the CNG charge is assumed homogenous in the combustion chamber for simplicity.

Combustion Model

Detailed Chemical Kinetics Model was used both to initiate flame propagation from spark energy in case of SI-CNG engine and for auto-ignition of diesel pilot in case of dual-fuel. For modeling of the flame propagation after ignition, G-equation model is used with the detailed chemistry model. Detailed chemistry model was used in both burned and unburned region which are governed by the positive and negative values of G scalar respectively. In short flame surface tracked by the G-equation divides the combustion chamber into three regions, burnt region inside the flame surface, unburnt region outside the flame surface and the flame itself. For SI engine combustion simulation instead of providing scalar G value to initiate G-equation model, spark energy was used to model the effect of spark. Spark energy was distributed evenly along the line (comprises 500 points) between the two spark-plug nodes. Also the spark temperature was set-up to be 5000 K. To get optimum results from spark ignition 20,000 cell mesh was used in a close proximity surrounding the spark plug. G-equation tracks the location of the turbulent flame by solving equation (1) using level set numerical method [26][27]

$$\frac{\partial \rho \tilde{G}}{\partial t} + \frac{\partial \rho \hat{u}_i \tilde{G}}{\partial x_i} = -D_t \kappa \left|\frac{\partial \tilde{G}}{\partial x_i}\right| + \rho_u S_t \left|\frac{\partial \tilde{G}}{\partial x_i}\right| \quad (1)$$

Where ρ_u is the unburned density, G is a non-reacting scalar and turbulent diffusion term is given by $D_t = \frac{C}{S_c}\frac{k^2}{\varepsilon}$, where k is the turbulent kinetic energy and ε is the turbulent dissipation.

Where S_t is the turbulent flame speed [28][29] and is calculated using equation (2).

$$S_t = S_l + u' \left\{ \left[\left(\frac{a_4 b_3^2}{2 b_1} Da \right)^2 + a_4 b_3^2 Da \right]^{\frac{1}{2}} \right\} \quad (2)$$

S_l is the laminar flame speed, u is the root mean square of the turbulent fluctuating velocity, $a_4 = 0.78$ [28], $b_1 = 2.0$ [30], $b_3 = 1.0$[31]. Da is Damkohler number.

$$Da = \frac{S_l l_t}{u\, l_F}$$

Laminar flame speed was calculated using the Gulder's coefficients for methane and taking laminar flame speed as reference turbulent flame speed was computed.

The turbulent thickness of the flame can be calculated by using the length scale of the turbulent flow and is given by equation (3)

$$l_t = c_\mu \frac{k^{3/2}}{\varepsilon} \text{ where } c_\mu = 0.47 \text{ [26]} \quad (3)$$

Diesel dual-fuel engine combustion comprises of auto-ignition and flame propagation modes. To model diesel auto-ignition detailed chemistry model was used and as the pilot quantity of the diesel is being burnt the G-equation model for flame propagation was turned on. Maximum temperature reached due to the auto-ignition of the pilot diesel quantity was noted in first simulation run and this temperature is used to trigger the G-equation.

Spray Modeling

For spray modeling KH-RT [32] breakup model was used with initial 50,000 parcels per nozzle. The primary breakup length was calculated using KH-ACT [33] model which takes into account aerodynamics, cavitation and turbulence effects.

Downloaded from SAE International by Wayne State University, Friday, September 16, 2016

Table 6. Spray Modeling Parameters.

KH size constant	0.6
KH velocity constant	0.188
KH time constant	7.0
RT size constant	0.1
RT time constant	1.0
Number of Injected parcels	300,000
Diffusivity factor, d_0	3.74e-006
Diffusivity exponent, n	1.6

Results and Discussion

Diesel-CNG Dual-fuel Engine Combustion

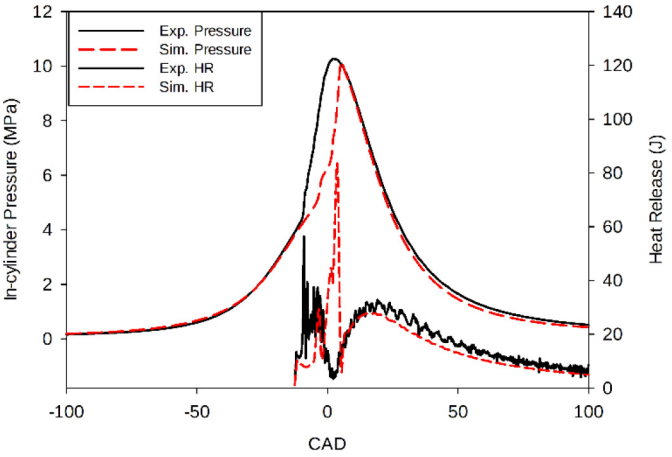

Figure 1. Mean Cylinder Pressure for SOI 23 BTDC Detailed chemistry is ON for G>0 (Burnt Zone)

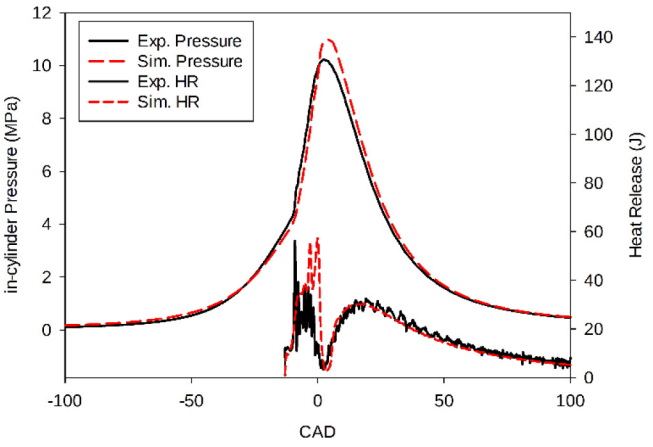

Figure 2. Mean Cylinder Pressure for SOI 23 bTDC

Figure 1, 2, 3 show the comparison of predicted and measured incylinder pressure for different start of injection (SOI) timings. It is evident from both simulation and experiment that the combustion characteristics of the diesel dual-fuel engine are very sensitive to the injection timing and pilot fuel quantity. In Figure 1 detailed chemistry is ON just in the burnt portion (inside of the flame) defined by G>0. Heat release rate is slower and under-predicted, compared to the case in Figure 2 when detailed chemistry is unburned on in both burnt and unburnt zones. Figure 1 show a much choppy heat release, due to chemical reactions taken place at various computational cell locations inside the burnt zone only.

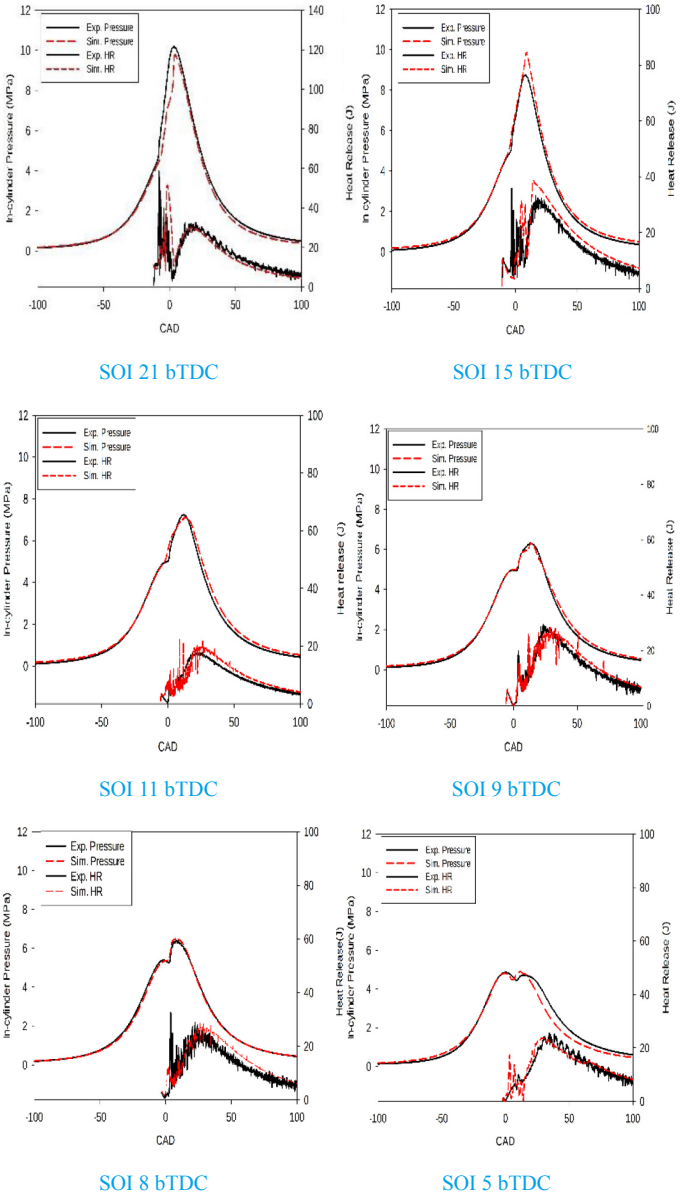

Figure 3. Mean Pressure for SOI 21 to 5 CA bTDC

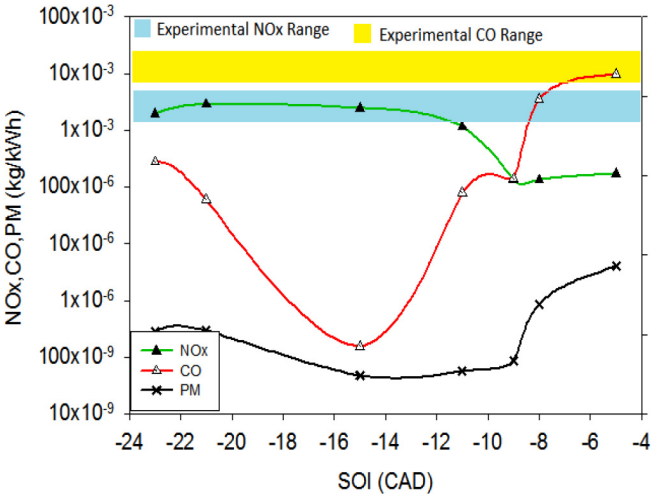

Figure 4. Emission Data from Simulations of Dual-fuel Engine

Downloaded from SAE International by Wayne State University, Friday, September 16, 2016

The simulated heat release traces shown in this paper are all unfiltered, to demonstrate this effect, which could be the artifact of the applying chemical kinetics in a Reynolds-Averaged Navier-Stokes Solver (RANS) with stochastic discrete particle spray injection sub model. The combustion phasing in these Dual-Fuel cases are very well predicted using the current approach of combined combustion model of detailed chemistry and G-equation as shown in agreement between the experimental cycle-averaged data of cylinder pressure. In particular, in the SOI 8 bTDC case as shown in Figure 3 where the pilot quantity of the diesel is increased to observe change in the combustion characteristic and is used in this work to validate the simulation result. Nevertheless, the combustion model generally underestimates slightly the ignition delay for dual-fuel combustion; hence results in the smooth transition from auto-ignition to the flame propagation dominated combustion. In some cases in Figure 3 the predicted pressure rise after auto ignition of the diesel pilot is more than that obtained from the experimental data. One reason is that G-equation model generally predicts faster reaction rate than the detailed chemistry model and hence it overestimates the turbulent flame speed. Also AHRR is over estimated by the detailed chemistry model, hence high rate of heat release is observed sometimes. As the injection timing is delayed, rate of heat release is decreased (SOI 8, 5 bTDC).

With the chemical kinetics, the pollutant emissions can also be predicted. As shown in Figure 4 experimental NO_x range [21] coincides with NO_x data obtained from the simulation for earlier SOI cases from 23 to 11 bTDC. Predicted NO_x is less than the experimental data for later injection events. CO emission measurement range from the experiment is higher than the predicted CO, primarily because of the homogeneous charge assumption used in the current dual-fuel simulations. Still late injection events agrees well with the experimental data.

The effect of pilot SOI timing on the emission can sometimes be inferred from the auto ignition timing and the spray penetration. As shown in Figure 5 the penetration length of the spray for different SOI timing, later injections show more distance travelled by the spray compared to the earlier injections. In Figure 4 emission data from simulation of the dual-fuel engine showed that the minimum CO and PM levels are obtained for SOI at 15 CA bTDC and minimum NO_x level for SOI at 5 CA bTDC. For later injections CO and PM tend to increase due to less time for the mixing and auto-ignition of the diesel spray. For SOI 15 CA bTDC highest NO_x levels are observed are associated with the high rate of heat release.

The combustion regime is divided into 3 zones, flame front, volume inside the flame-front and volume outside the flame-front. Flame is always modelled at chemical equilibrium. Species like NO, N, N_2O and NO_2 are not included in the in the flame modelling because of their relatively short resident time within the flame front and relative slow chemical reaction rate of NO_x producing reactions. [34] These species are calculated at the burnt zone using detailed chemistry model. As the detailed chemistry model is also working outside the flame front, this modelling is helpful in knock detection and hence can be used for the simulation of PREMIER dual-fuel combustion mode. Figure 6 shows a temperature profile in dual-fuel combustion process for SOI 23 CA bTDC in which the high temperature zones are forming in between the spray streams while the spray is advancing in the chamber. The highest temperature zone is for each spray towards the swirl and almost at the middle section of the spray cone. Advances of the counters for 2000 K line is followed by the less temperature 1700 K lines and flame front is inside the envelope of 1300 K lines. This regime is shown for the least concentration of the CH_4 gas in Figure 7 for the same CA. It shows the iso-surface for the maximum mass fraction of CH_4 and predicts the low concentration of fuel in the regimes between the two spray clouds which are the burnt zones and contains maximum temperature gases. The same regime in Figure 8 is shown to have the highest temperature of the droplets (736 K) and is also the site of G=0 flame front. At the end of the spray new hot spot gets created near the tail of the spray. In this simulation only one flame surface is being tracked by equation (1) and it is established at the point where the auto-ignition happens for the first time.

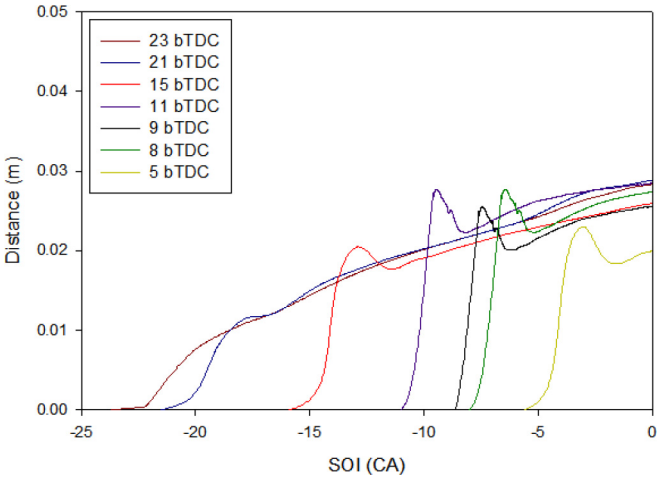

Figure 5. Penetration Length of the Spray for Different SOI

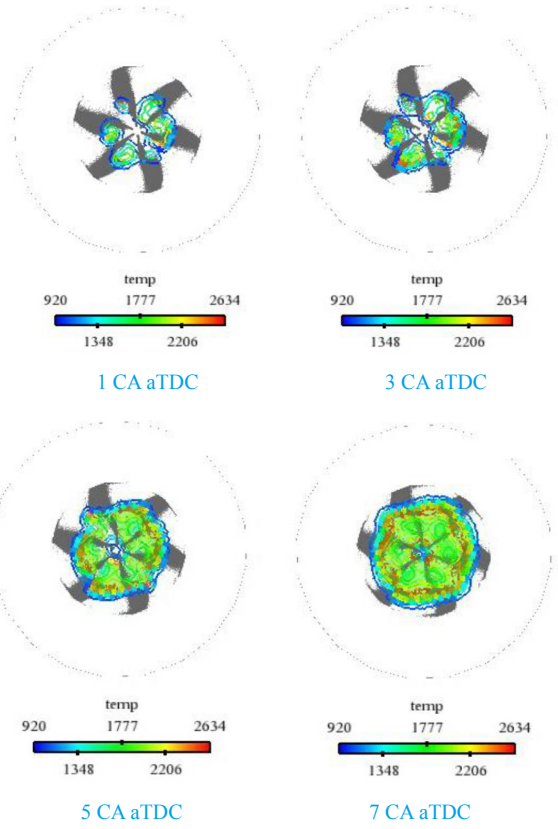

Figure 6. Temperature profile in dual-fuel combustion process for SOI 23 CA bTDC

Downloaded from SAE International by Wayne State University, Friday, September 16, 2016

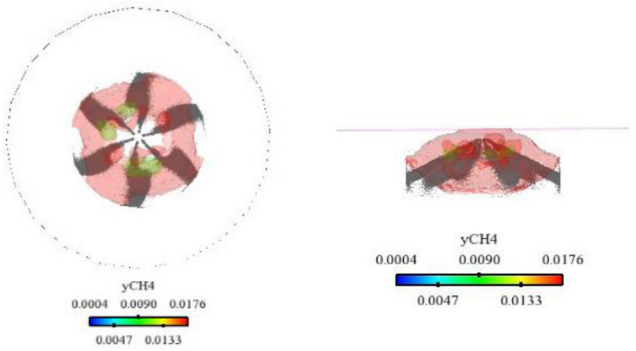

1 CA aTDC

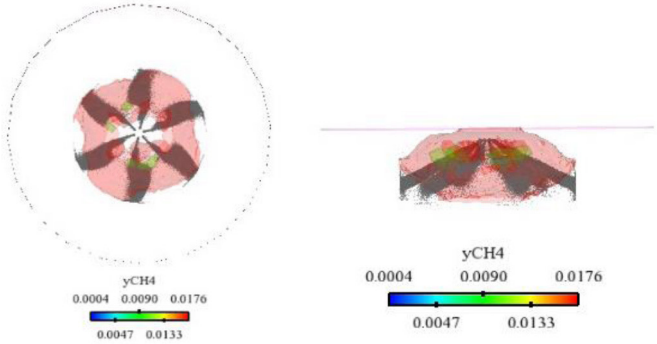

3 CA aTDC

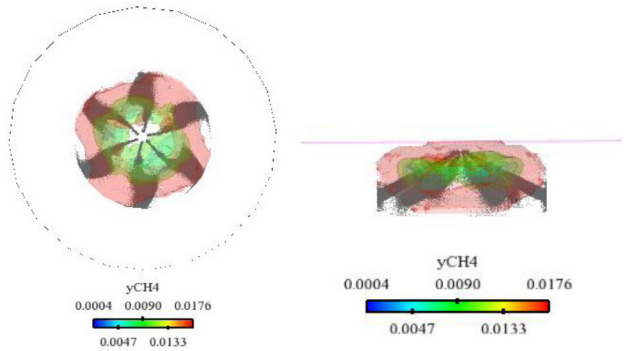

5 CA aTDC

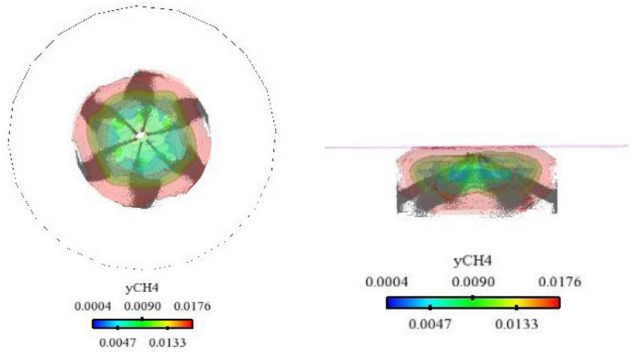

7 CA aTDC

Figure 7. Profile of minimum mass fraction of CH_4 depicting transition from auto-ignition to the flame propagation dominated combustion for SOI 23 bTDC

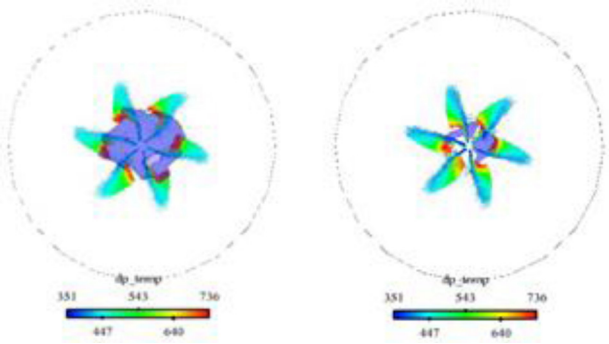

4bTDC 2bTDC

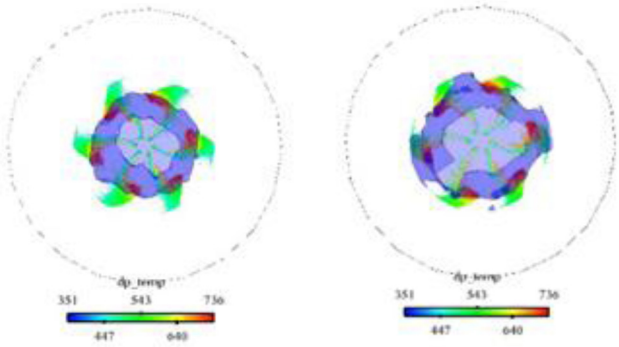

2aTDC 5aTDC

Figure 8. Profile of scalar G=0 and droplet temperature

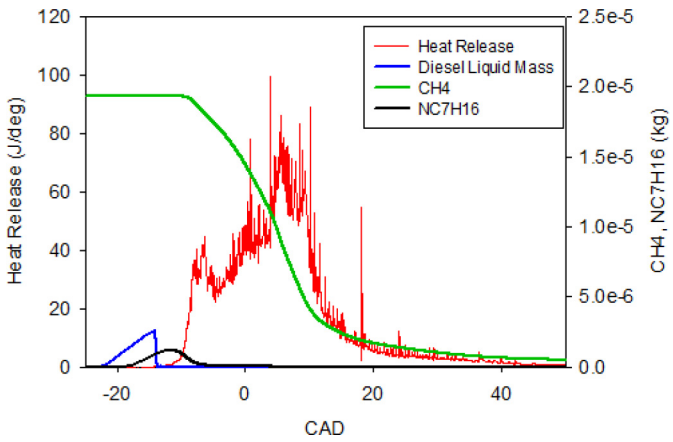

Figure 9. Heat release and consumption of fuel species for SOI 23 bTDC

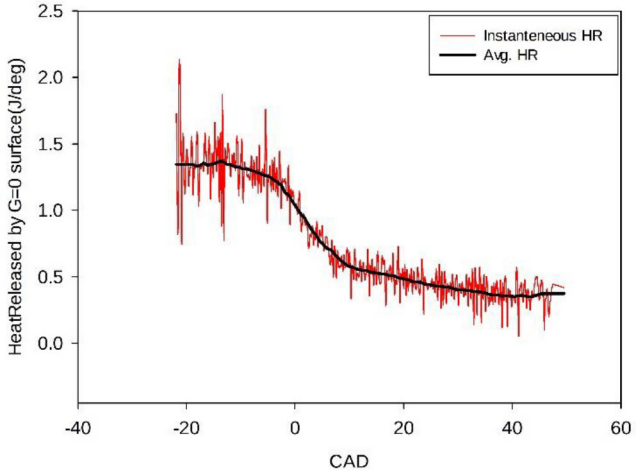

Figure 10. Instantaneous Heat Released by G=0 surface for SOI 23 CA bTDC

Downloaded from SAE International by Wayne State University, Friday, September 16, 2016

Figure 9 shows the unfiltered chemical heat release in J/deg from different modes of combustion. The first peak of heat release significantly shows the auto-ignition of the diesel pilot fuel quantity. The distance between first two peaks show the transition period from auto-ignition to the flame propagation type combustion. Simultaneously it shows the reduction in the CH_4 concentration. The fluctuating nature of the heat release curve is partially due to numerical aspect of the simulation but mostly due to the uneven simultaneous endothermic and exothermic combustion reactions.

Figure 10 shows the heat release only in the flame thickness which is tracked by solving G-equation for non-reactive G(x, t) scalar. The turbulent flame thickness was calculated by using equation (3). As per the combustion modeling used in this paper, the flame thickness region is assumed to have a chemical equilibria and hence detailed chemistry model do not work in the small thickness (order of 0.5 mm) of the turbulent flame. Comparing the heat released by equilibrium turbulent flame to the total chemical heat released (Figure 9) it shows that contribution to total combustion of G surface is very small, but is play a very important role of separating unburnt and burnt zones. This feature is very useful in cases of end-gas autoignition or to predict knock. In case of a knocking combustion thinning of the turbulent flame is expected in this particular model. Usually detailed chemistry model slows down the G-equation flame propagation by increasing dilution factor in the unburnt zone.

Figure 11 shows the iso-surface to visualize flame front for the SOI 15 CA bTDC case. As the first image shows the highest temperature (2000 K) occurs in the direction of the swirl and establishes a flame surface at a very fast speed. The general structure of this flame is dome shape at the beginning and becomes more spherical as it grows and is being quenched at the surface (cylinder head and bawl walls) as the conjugate heat transfer model is working at the walls and reduces the temperature of the flame surface. Also when spray hits the wall few droplets form a thin layer of the wall film and other droplets depending on the weber number of the individual droplet and its direction bounces off the wall. This setup helps in the prediction of the soot and unburned hydrocarbon prediction.

4.77bTDC 3.5bTDC

1.34bTDC 2.2aTDC

Figure 11.

5.88aTDC 8.99aTDC

Figure 11 (cont.). Temperature profile (2000 K) in dual-fuel combustion process for SOI 15 BTDC

PREMIER (PREmixed Mixture Ignition in the End-gas Region) Combustion in Dual Fuel Engine

In PREMIER combustion mode first mode of heat release is due to the flame propagation and the second mode consist of the autoignition like combustion of mixed fuel in the end gas region. This combustion mode is also like a very light knocking, low temperature combustion. The same simulation strategy was used for this mode of dual-fuel combustion also. As the detailed chemistry model is ON outside of the flame, in this combustion mode it helps to detect knock. The pre-flame chemistry is very important in this case. Two cases are simulated and compared in this paper which are shown in Figure 12 and Figure 13. For these two cases as per the experimental conditions only pure CH_4 is used as a gaseous fuel. Table 7 shows the specifications of the supercharged CI engine.

Table 7. Experimental Condition for PREMIER Combustion [35][36]

Engine Type	4-stroke, single-cylinder, water cooled
Bore x Stroke	96 x 108 mm
Swept Volume	781.7 cm^3
Compression Ratio	16
Combustion System	Dual-fuel, Direct Injection
Engine Speed	1000 rpm
Intake Pressure	200 kPa
Pilot fuel injection pressure	40 MPa
Pilot fuel injection quantity	3 mg/cycle
Nozzle hole x diameter	3x0.10mm
EGR	none

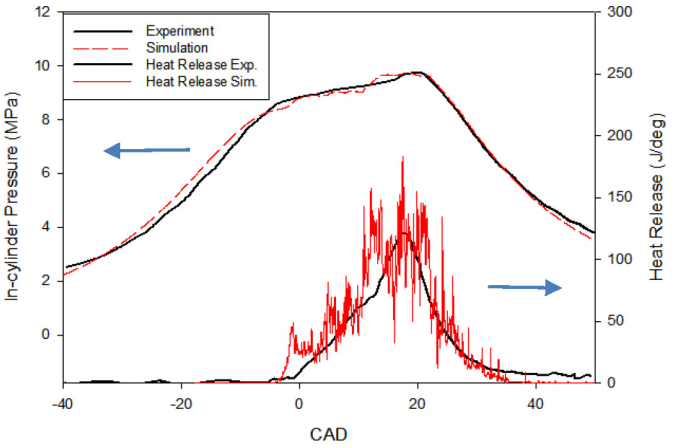

Figure 12. Mean Cylinder Pressure for SOI 4.5 CA bTDC

Downloaded from SAE International by Wayne State University, Friday, September 16, 2016

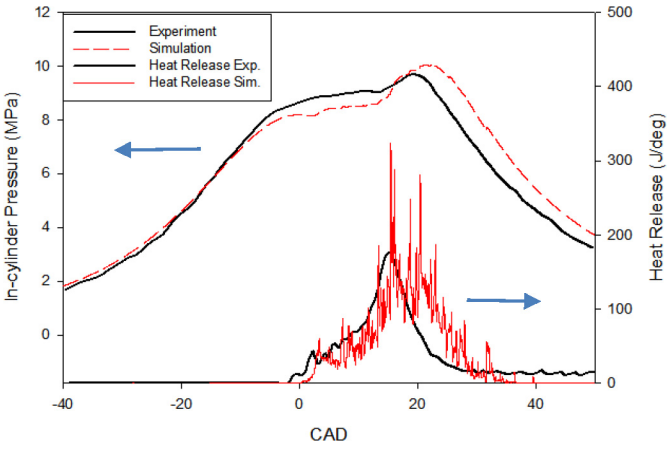

Figure 13. Mean Cylinder Pressure for SOI 2.5 CA bTDC

Highly fluctuating heat release values represent the pre-flame chemistry at work. Most of the pre-flame region is relatively cooler than the burn region with few droplets of diesel evaporating and a very lean mixture of air and CH_4 and hence reactions occurring in this region are endothermic in nature.

SI-CNG Engine

In this paper for SI engine focus is on the ignition energy requirements of CNG when using different air-fuel ratios. By varying the ignition energy, the effects on combustion are observed. Advanced ignition system design and operation may impact engine combustion [37, 38, 39].

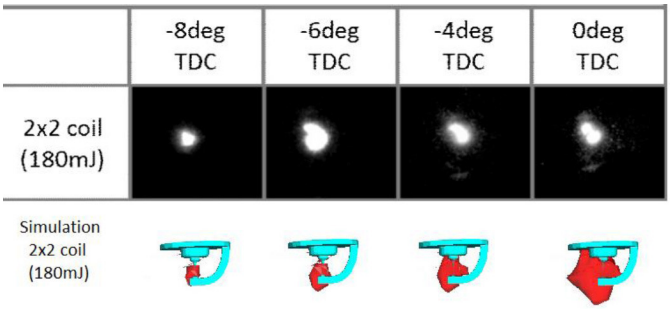

Figure 14. Spark Energy Visualization at λ = 1.25 from Simulation 2×2 coil 180mJ (G=0 iso-surface represent CH_4 burning zone)

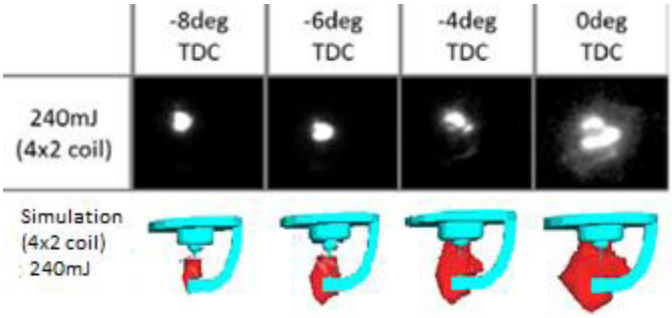

Figure 15. Spark Energy Visualization at λ = 1.25 from Simulation 4×2 coil 240mJ (G=0 iso-surface represent CH_4 burning zone)

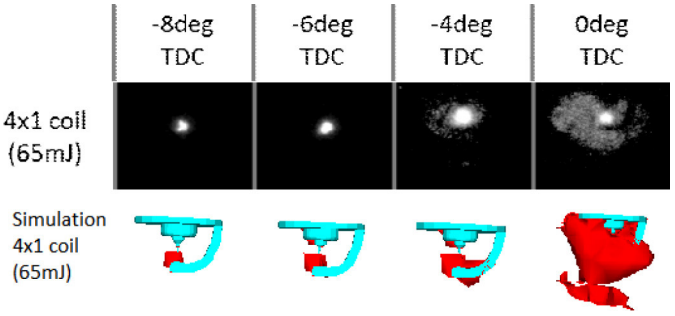

Figure 16. Spark Energy Visualization at λ = 0.9from Simulation 4×1 coil 65mJ (G=0 iso-surface represent CH_4 burning zone)

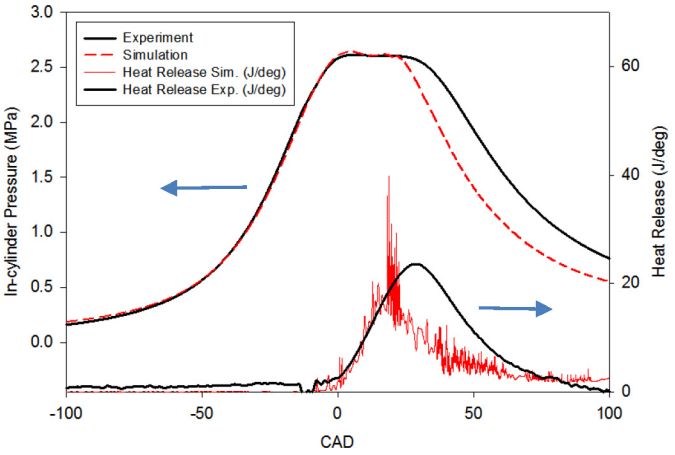

Figure 17. Mean Cylinder Pressure for λ = 1.25 and 180 mJ Spark Energy

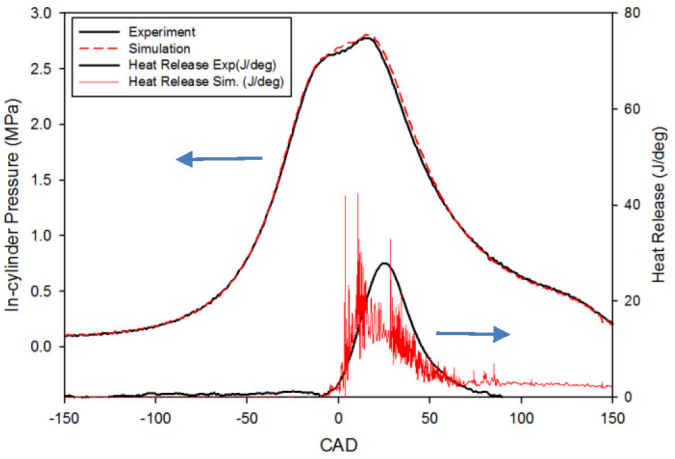

Figure 18. Mean Cylinder Pressure for λ = 1.25 and 240 mJ Spark Energy

Figure 14, 15, 16 shows the kernel growth at the start of the combustion due to the spark in 3D CFD. The start of the flame from the tips of the spark plug is clearly described in these images. The spark kernel is the iso-surface G=0 got by solving equation (1). The white spots on the black background is the visible light image of the spark kernel growth. These images are taken by the endoscope through the right side of the spark plug. The red iso-surface show the G=0 surface which is colored by the CH_4 concentration. This is the outer surface of the flame, inside this surface is the area of turbulent flame thickness and inside that flame is the burnt region with hot

Downloaded from SAE International by Wayne State University, Friday, September 16, 2016

gases going through the combustion process. Experimental images does not show the invisible spectrum of the flame, but just the visible light, hence the actual flame surface is larger by a very small amount than the white spot area. Current model setup of combustion simulation is capable of capturing the most of the kernel flame growth with high accuracy as shown in above figures for various spark plug energies and lean as well as slightly rich air fuel mixtures.

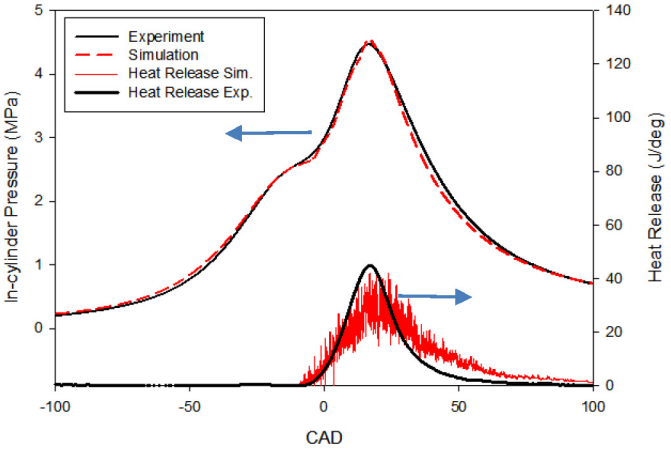

Figure 19. Mean Cylinder Pressure for λ = 0.9 and 180 mJ Spark Energy

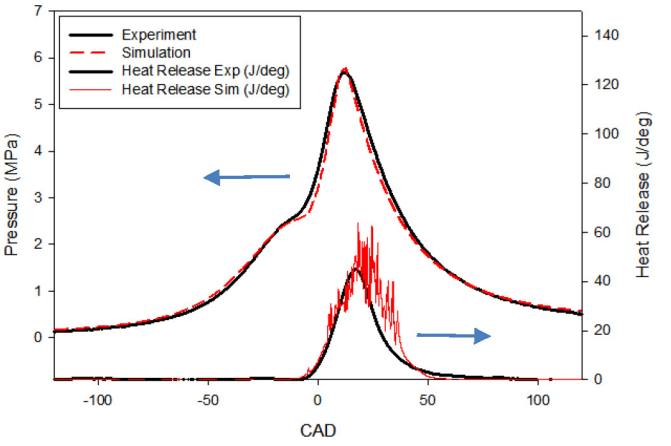

Figure 20. Mean Cylinder Pressure for λ = 0.9 and 240 mJ Spark Energy

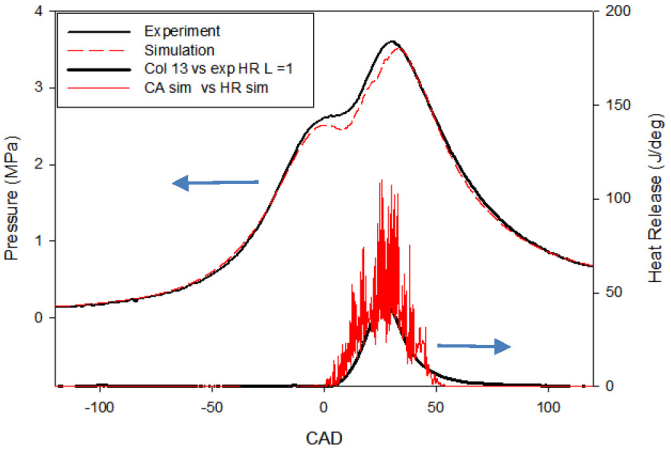

Figure 21. Mean Cylinder Pressure for λ = 0.9 and 65mJ Spark Energy

SI-CNG simulations for lean mixtures were performed. The G-equation model with detailed chemistry solver was used to describe the effect of the spark energy. Simulation shows similar trend in the visualization of the combustion start. As shown in Figure 17, for λ=1.25 and spark energy 180 mJ the combustion is faster than the experiment. On the contrary for λ = 1.25 and spark energy 240 mJ (Figure 18) in simulation combustion duration is more than the experiment. The experimental data is averaged over 100 combustion cycles but the simulation run is only one per case. Though the simulation is using time-averaged algorithms there is a slight mismatch in the heat release data when compared with the experimental data. This could be due to slight difference in the wall temperature and swirl ratio.

The pressure obtained from this model is higher than the experimental peak pressure. But for higher equivalence ratio λ=0.9 and same spark energy 180 mJ model prediction of the pressure and heat release is better compared to the previous cases. For higher spark energy 240 mJ though heat release rate is higher than the experimental measurements. As shown in Figure 21, 65 mJ is the least amount of energy used in simulation, below 60 mJ spark energy combustion is unstable and mostly incomplete. Simulation of λ=0.9 and spark energy 65 mJ took the large amount of time to finish compared to the previous cases. This is mostly due to a level of refinement required for the initial flame propagation to setup after the spark event. The reason for the higher rate of heat release in the model should be investigated. Model should have to be redefined for the correct turbulent flame speed. Figure 22 shows the effect spark energy on IMEP for different air-fuel ratios. For lean mixtures 240 mJ spark energy shows improvement over 180 mJ energy.

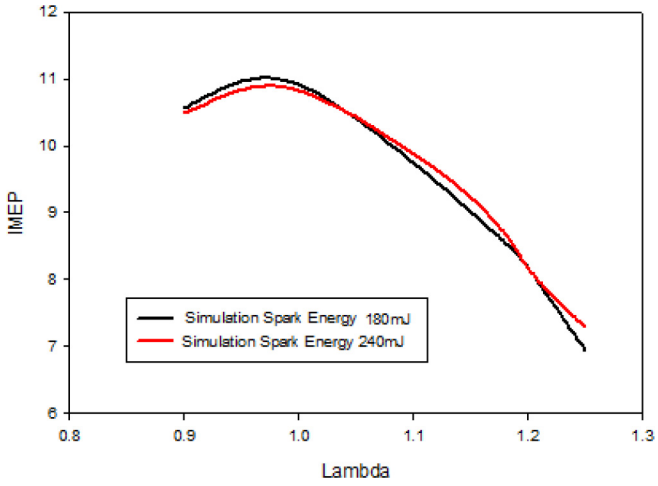

Figure 22. Effect of Spark Energy on IMEP

Downloaded from SAE International by Wayne State University, Friday, September 16, 2016

Conclusion

For the diesel dual-fuel and SI engine numerous simulations were performed and results were compared with the experimental data. Conclusions of these simulations are as follows:

1. Coupling of detailed chemistry model and G-equation models is the optimum way to simulate the diesel dual-fuel engine combustion. Currently G equation model tracks the flame propagation once the temperature reaches to 1800 K in any cell and G=0 surface can be initialized only once. Model has to be developed further to use more than one fuel and multiple initializations of G=0 surface so that the transition from the auto-ignition of diesel to flame propagation dominated combustion of CNG can be described effectively.
2. Two strategies were used to model the duel fuel combustion. In first attempt G-equation was turned on right after the injection event is finished. In this case for SOI 5 CA bTDC there was an overestimated ignition delay. Hence in second attempt G-equation model was turned on before the pilot injection event. Also the detailed chemistry was activated in the burnt zone as well as outside the flamelet (unburnt zone). Due to this strategy ignition delay was reduced for late injection events as for SOI 8 and 9 CA bTDC cases.
3. For early injection events both strategies are lacking accuracy to predict ignition delay possibly due to G surface propagation model.
4. PREMEIR combustion with nearly knocking properties can be predicted with this current model and the heat release rate is also comparable with the experimental studies. Hence the same model can be used to predict knock in the diesel dual-fuel operation.
5. For SI engine lean charge was ignited using different spark energies. Author was able to get satisfactory results only for 180mJ and 240 mJ spark energy using GRI mechanism and LLNL CH_4 mechanism was unable to give satisfactory results. For less spark energy than 65 mJ simulation was too sensitive to the grid density and the initial turbulent boundary condition and results were inconclusive. Precise modelling and further work is needed to simulate the effect of spark energy in SI lean burn engine as flame propagation model needs tuning each time spark energy is changed.
6. Summarizing all the results from three different simulation namely diesel-CNG dual-fuel combustion, PREMIER combustion and SI combustion with variable spark energy can be modelled using detailed chemistry and G-equation together.

References

1. Wagemakers, A. and Leermakers, C., "Review on the Effects of Dual-Fuel Operation, Using Diesel and Gaseous Fuels, on Emissions and Performance," SAE Technical Paper 2012-01-0869, 2012, doi:10.4271/2012-01-0869.
2. Selim, M.Y.E., “Effect of engine parameters and gaseous fuel type on the cyclic variability of dual fuel engines,” *Fuel* 84(7-8):961-971, 2005, doi:10.1016/j.fuel.2004.11.023.
3. Elnajjar, E., Selim, M.Y.E., and Hamdan, M.O., “Experimental study of dual fuel engine performance using variable LPG composition and engine parameters,” *Energy Convers. Manag.* 76:32-42, 2013, doi:10.1016/j.enconman.2013.06.050.
4. Sahoo, B.B., Sahoo, N., and Saha, U.K., “Effect of engine parameters and type of gaseous fuel on the performance of dual-fuel gas diesel engines-A critical review,” *Renew. Sustain. Energy Rev.* 13(6-7):1151-1184, 2009, doi:10.1016/j.rser.2008.08.003.
5. Papagiannakis, R.G., Rakopoulos, C.D., Hountalas, D.T., and Rakopoulos, D.C., “Emission characteristics of high speed, dual fuel, compression ignition engine operating in a wide range of natural gas/diesel fuel proportions,” *Fuel* 89(7):1397-1406, 2010, doi:10.1016/j.fuel.2009.11.001.
6. Zoldak, P., Sobiesiak, A., Bergin, M., and Wickman, D., "Computational Study of Reactivity Controlled Compression Ignition (RCCI) Combustion in a Heavy-Duty Diesel Engine Using Natural Gas," SAE Technical Paper 2014-01-1321, 2014, doi:10.4271/2014-01-1321.
7. Zoldak, P., Sobiesiak, A., Wickman, D., and Bergin, M., "Combustion Simulation of Dual Fuel CNG Engine Using Direct Injection of Natural Gas and Diesel," *SAE Int. J. Engines* 8(2):846-858, 2015, doi:10.4271/2015-01-0851.
8. Papagiannakis, R.G., “Study of air inlet preheating and EGR impacts for improving the operation of compression ignition engine running under dual fuel mode,” *Energy Convers. Manag.* 68:40-53, 2013, doi:10.1016/j.enconman.2012.12.019.
9. Papagiannakis, R.G., Hountalas, D.T., and Rakopoulos, C.D., “Theoretical study of the effects of pilot fuel quantity and its injection timing on the performance and emissions of a dual fuel diesel engine,” *Energy Convers. Manag.* 48(11):2951-2961, 2007, doi:10.1016/j.enconman.2007.07.003.
10. Kong, S., Han, Z., and Reitz, R., "The Development and Application of a Diesel Ignition and Combustion Model for Multidimensional Engine Simulation," SAE Technical Paper 950278, 1995, doi:10.4271/950278.
11. Zhang, Y., Kong, S., and Reitz, R., "Modeling and Simulation of a Dual Fuel (Diesel/Natural Gas) Engine With Multidimensional CFD," SAE Technical Paper 2003-01-0755, 2003, doi:10.4271/2003-01-0755.
12. Kong, S.-C. and Reitz, R.D., “Multidimensional Modeling of Diesel Ignition and Combustion Using a Multistep Kinetics Model,” *J. Eng. Gas Turbines Power* 115(4):781-789, 1993.
13. Liang, L. and Reitz, R., "Spark Ignition Engine Combustion Modeling Using a Level Set Method with Detailed Chemistry," SAE Technical Paper 2006-01-0243, 2006, doi:10.4271/2006-01-0243.
14. Liang, L., Reitz, R., Iyer, C., and Yi, J., "Modeling Knock in Spark-Ignition Engines Using a G-equation Combustion Model Incorporating Detailed Chemical Kinetics," SAE Technical Paper 2007-01-0165, 2007, doi:10.4271/2007-01-0165.
15. Long, L., “Multidimensional Modeling of Combustion and Knock in Spark-Ignition Engines with Detailed Chemical Kinetics,” University of Wsconsin-Madison, 2006.

Downloaded from SAE International by Wayne State University, Friday, September 16, 2016

16. Abagnale, C., Cameretti, M.C., Simio, L. De, Gambino, M., Iannaccone, S., and Tuccillo, R., "Numerical simulation and experimental test of dual fuel operated diesel engines," *Appl. Therm. Eng.* 65(1-2):403-417, 2014, doi:10.1016/j.applthermaleng.2014.01.040.
17. Stringer F.W., Clarke A.E., and C.J.S., "The spontaneous ignition of hydrocarbon fuels in a flowing system," *Proc. Instn. Mech. Engrs* 184:212-225.
18. Magnussen, B.F. and Hjertager, B.H., "On mathematical modeling of turbulent combustion with special emphasis on soot formation and combustion," *Symp. Combust.* 16(1):719-729, 1977, doi:10.1016/S0082-0784(77)80366-4.
19. Nicol, D.G., Malte, P.C., Hamer, a. J., Roby, R.J., and Steele, R.C., "Development of a Five-Step Global Methane Oxidation-NO Formation Mechanism for Lean-Premixed Gas Turbine Combustion," *J. Eng. Gas Turbines Power* 121(2):272, 1999, doi:10.1115/1.2817117.
20. Mattarelli, E., Rinaldini, C.A., and Golovitchev, V.I., "CFD-3D analysis of a light duty Dual Fuel (Diesel/Natural Gas) combustion engine," *Energy Procedia* 45:929-937, 2014, doi:10.1016/j.egypro.2014.01.098.
21. Yang, B., Wei, X., Xi, C., Liu, Y., Zeng, K., and Lai, M., "Experimental study of the effects of natural gas injection timing on the combustion performance and emissions of a turbocharged common rail dual-fuel engine," *Energy Convers. Manag.* 87:297-304, 2014, doi:10.1016/j.enconman.2014.07.030.
22. Polcyn, N., Lai, M., and Lee, P., "Investigation of Ignition Energy with Visualization on a Spark Ignited Engine powered by CNG," 2014, doi:10.4271/2014-01-1331.Copyright.
23. n-Heptane, Detailed Mechanism, Version 3.1, https://combustion.llnl.gov/mechanisms/alkanes/n-heptane-detailed-mechanism-version-3, 2011.
24. Mehl, M., Pitz, W., Sjöberg, M., and Dec, J., "Detailed Kinetic Modeling of Low-Temperature Heat Release for PRF Fuels in an HCCI Engine," SAE Technical Paper 2009-01-1806, 2009, doi:10.4271/2009-01-1806.
25. Gregory P. Smith, David M. Golden, Michael Frenklach, Nigel W. Moriarty, Boris Eiteneer, Mikhail Goldenberg, Bowman C. Thomas, Ronald K. Hanson, Soonho Song, William C. Gardiner, Jr., Vitali V. Lissianski, and Z.Q., "GRI-Mechanism 3.0," http://combustion.berkeley.edu/gri-mech/version30/text30.html.
26. Ewald, J. and Peters, N., "A Level Set Based Flamelet Model for the Prediction of Combustion in Spark Ignition Engines Unsteady Premixed Combustion Model," *Int. Multidimens. Engine Model. User's Gr. Meet.* 1-6, 2005.
27. Tan, Z. and Reitz, R., "Modeling Ignition and Combustion in Spark-ignition Engines Using a Level Set Method," SAE Technical Paper 2003-01-0722, 2003, doi:10.4271/2003-01-0722.
28. Burning, T., Author, V., Source, B., Royal, T., and Stable, S., "Studies of the Turbulent Burning Velocity," *Math. Phys. Sci.* 431(1882):315-335, 1990.
29. Turns, S.R., "An Introduction to Combustion-Concepts and Applications," McGraw-Hill, Inc., New York, 1996.
30. A TWO-EDDY PREMIXED TURBULENT THEORY OF FLAME PROPAGATION, 301(1457):1-25, 1980.
31. Damkohler, G., "THE EFFECT OF TURBULENCE ON THE FLAME VELOCITY IN GAS MIXTURES," *Zei Tschrift Fur 'Elektrochemie Und angev18ndte pr.ysika1ische Chemie.* 46(November), 1940, doi:10.1097/00152192-198911000-00004.
32. Reitz, R.D., "Modeling Atomization Processes in High-Pressure Vaporizing Sprays," *At. Sprays* 3:309-337, 1987.
33. Som, S. and Aggarwal, S.K., "Effects of primary breakup modeling on spray and combustion characteristics of compression ignition engines," *Combust. Flame* 157(6):1179-1193, 2010, doi:10.1016/j.combustflame.2010.02.018.
34. Liang, L., Reitz, R.D., Yi, J., and Iyer, C.O., "A G -equation Combustion Model Incorporating Detailed Chemical Kinetics for PFI / DI SI Engine Simulations G -equation description of turbulent," 2006.
35. Azimov, U., Tomita, E., and Kawahara, N., "Ignition, Combustion and Exhaust Emission Characteristics of Micro-pilot Ignited Dual-fuel Engine Operated under PREMIER Combustion Mode," 2011.
36. Aksu, C., Kawahara, N., Tsuboi, K., and Nanba, S., "Effect of Hydrogen Concentration on Engine Performance, Exhaust Emissions and Operation Range of PREMIER Combustion in a Dual Fuel Gas Engine Using Methane-Hydrogen Mixtures," JSAE 20159, 2015.
37. Lee, M.J., Hall, M., Ezekoye, O. a, and Matthews, R., "Voltage, and Energy Deposition Characteristics of Spark Ignition Systems Reprinted From : SI Combustion and Direct Injection SI Engine Technology," (724), 2005.
38. Lee, Y. and Boehler, J., "Flame Kernel Development and its Effects on Engine Performance with Various Spark Plug Electrode Configurations," SAE Technical Paper 2005-01-1133, 2005, doi:10.4271/2005-01-1133.
39. Alger, T., Mangold, B., Mehta, D., and Roberts, C., "The Effect of Sparkplug Design on Initial Flame Kernel Development and Sparkplug Performance Reprinted From : SI Combustion and Direct Injection SI Engine Technology," (724), 2014, doi:10.4271/2006-01-0224.

ACKNOWLEDGEMENT

The software license support of Convergent Science is highly appreciated. The helpful discussions with Prof. Tomita and Prof. Kawahara on PREMIER cases are also acknowledged.

NOMENCLATURE

λ - Air -Fuel Equivalence Ratio

aTDC - after Top Dead Center

bTDC - before Top Dead Center

BMEP - Break Mean Effective Pressure

CAD - Crank Angle Degree

CI - Compression Ignited

CFD - Computational Fluid Dynamics

Downloaded from SAE International by Wayne State University, Friday, September 16, 2016

CO - Carbon Monoxide

CNG - Compressed Natural Gas

ECU - Electronic Control Unit

IMEP - Indicated Mean Effective Pressure

HC - Hydrocarbon Emissions

LLNL - Lawrence Livermore National Laboratory

NG - Natural Gas

NO - Nitrogen Oxide

NO_x - Nitrogen Oxides Emissions

PM - Particulate Matter

PREMIER - PREmixed Mixture Ignition in the End-gas Region

SI - Spark Ignited

SOI - Start of Injection

The Engineering Meetings Board has approved this paper for publication. It has successfully completed SAE's peer review process under the supervision of the session organizer. The process requires a minimum of three (3) reviews by industry experts.

All rights reserved. No part of this publication may be reproduced, stored in a retrieval system, or transmitted, in any form or by any means, electronic, mechanical, photocopying, recording, or otherwise, without the prior written permission of SAE International.

Positions and opinions advanced in this paper are those of the author(s) and not necessarily those of SAE International. The author is solely responsible for the content of the paper.

ISSN 0148-7191

http://papers.sae.org/2016-01-0789